

MIKROKOPTER DOCUMENTATION

CYPHY LABORATORY

Inkyu Sa

October 31, 2011

Contents

I. Introduction	3
A. Purpose	3
B. Coordinate systems	3
C. Position control	5
D. MK acceleration scale factor measurement	6
E. SI units and log message protocol	9
1. SI units	9
2. log message protocol	9
F. Complex dynamics of the MK quadrotor	11
G. System latency	12
H. Velocity estimation	15
1. X axis acceleration	15
2. Y axis acceleration	16
3. Z axis acceleration	17
I. ROS implementation	22
J. Yaw control	23
K. Altitude control	25
1. PID altitude control	26
L. Flight time calculation	26
M. Battery discharge dynamics	28
N. Platform price comparison.	28
O. Precision comparison	29
P. Ground truth and estimation.	30
1. VICON coordinate system and experiment setup	31
II. References	34
References	35

I. INTRODUCTION

A. Purpose

The objectives of this document are to create written history while implementing the quadrotor using Mikrokopter (MK). In addition it will be a good opportunity to share this knowledge with other researchers who are interested in using the MK platform.

B. Coordinate systems

The MK doesn't specify a scientific coordinate system. It only has pitch, roll and yaw angles. The red bar is the front and the opposite is the rear. Pitch (Nick) angle results in forwards and backwards movements. In contrast, roll angle results in left and right movements. When we push all the way up the pitch stick (right stick on mode2), "StickNick" value (516) is transmitted to the FlightControl(FC). This implies "moving forward with the fastest speed". It is the maximum value of pitch angle. When we pull all the way down the pitch stick, "StickNick" value (-592) is transmitted to the FC. This implies "moving backward with the fastest speed". On the other hand, when pushed all the way right, the roll stick, "StickRoll" value (-516) is transmitted to the FC. When pushed all the way left, the roll stick, "StickRoll" value (512) is transmitted to the FC. Commonly the forward direction is the x-axis of robots and the right direction is the positive y-axis. Pitch angle implies rotation around the y-axis and the roll angle implies rotation around x-axis according to the right-hand rule. Positive pitch angle causes the vehicle to move backwards- the opposite of MK notation. Positive roll angle causes it to move right-again the opposite of MK notation.



FIG. 1: The MK coordinate frame

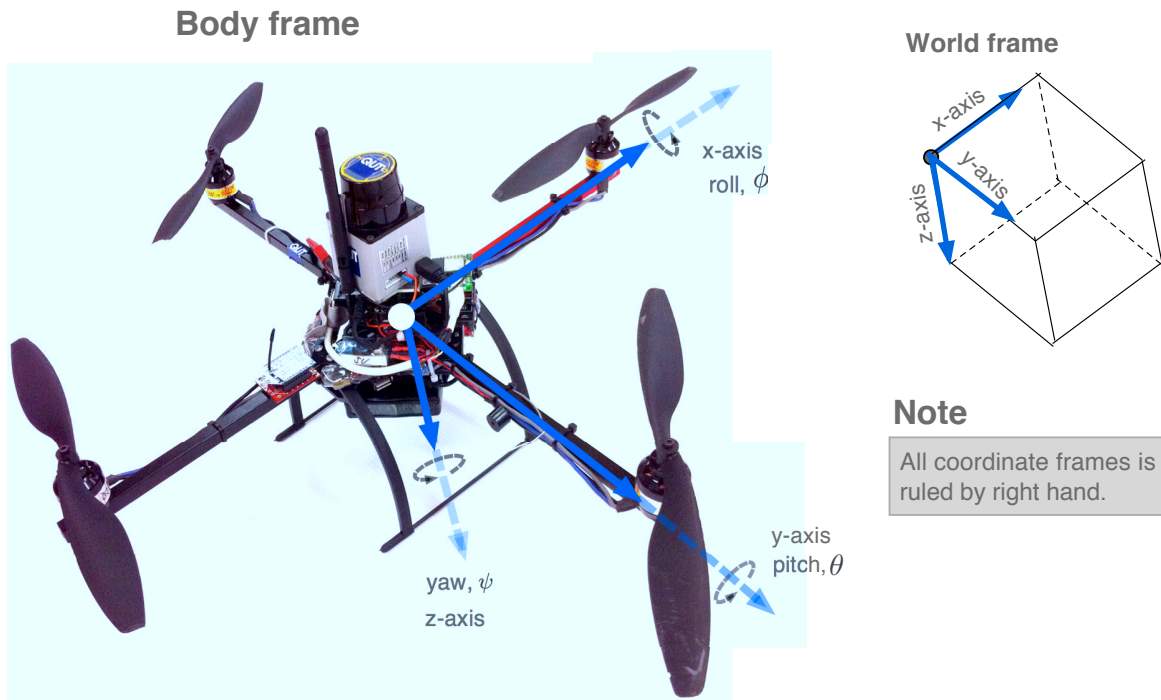


FIG. 2: The defined coordinate frame

C. Position control

In order to control the quadrotor, a traditional PD controller is implemented. The inputs for the controller are desired position and velocity and the outputs are pitch and roll commands. The laser range finder provides x,y positions and a yaw angle every 100ms and these PD controllers generate outputs at the same rate. The unit of the position and angle are represented in SI units, such as metres and radian.

$${}^W\theta^* = K_p({}^Wx^* - {}^Wx) + K_d \frac{d}{dt}({}^Wx^* - {}^Wx) \quad (1)$$

$${}^W\phi^* = K_p({}^Wy^* - {}^Wy) + K_d \frac{d}{dt}({}^Wy^* - {}^Wy) \quad (2)$$

${}^W\theta^*$ notes the pitch input in world frame and ${}^Wx^*$ is the reference input which the quadrotor should follow. Wx is the current position of the quadrotor in the world frame and this data is provided from the laser scan matcher. The desired output to the MK must be in the range ± 128 . Inputs are divided by the scale factor(120).

Then command angles are with respect to the world frame. The world and body frames are related by the yaw angle transformation.

$${}^B\mathbf{R}_W(\psi) = \begin{bmatrix} \cos \psi & -\sin \psi \\ \sin \psi & \cos \psi \end{bmatrix}, \quad (3)$$

where ψ is the angle of the world frame with respect to the body frame.

$$\begin{bmatrix} {}^B\theta^* \\ {}^B\phi^* \end{bmatrix} = \mathbf{R}(\psi) \cdot \begin{bmatrix} {}^W\theta^* \\ {}^W\phi^* \end{bmatrix} \quad (4)$$

Finally, the commands in the body frame are

$${}^B\theta^* = \cos \psi \cdot {}^W\theta^* - \sin \psi \cdot {}^W\phi^* \quad (5)$$

$${}^B\phi^* = \sin \psi \cdot {}^W\theta^* + \cos \psi \cdot {}^W\phi^* \quad (6)$$

Pitch	-90°	-60°	-50°	-45°	-15°	0°	15°	45°	50°	60°	90°
1st	602	522	458	428	152	0	-122	-431	-457	-531	-617
2nd	602	525	468	432	154	0	-123	-433	-462	-532	-618
3rd	602	523	470	422	153	0	-122	-432	-463	-532	-617
Mean	602	523.3	465.3	427.3	153	0	-122.3	-432	-460.6	-531.6	-617.3

TABLE I: MK AccNick Acceleration versus pitch true angle measurement ruled by right hand.

D. MK acceleration scale factor measurement

MK doesn't provide either SI units or documents explaining MK units. These data are unscaled measurements. Hence we try to figure out what the actual units are. This data is measured by an external accelerometer and MikroKopter Tool V1.72.

a. Pitch acceleration The contents of TABLE I are the pitch acceleration data from the MK. The unit of the measurement is unknown.

Fig. 3 shows the linear line fitting with the measured data. In the x-direction the equation of motion is

$$\ddot{x} = k \sin \theta \quad (7)$$

Where \ddot{x} refers to the acceleration data provided from MK quadrotor, k is the scale factor and θ is the pitch angle. Finally, $k = 606.3 \text{ units}/g$ can be calculated and the acceleration value also can be obtained in units of $1g$.

b. Roll acceleration The contents of TABLE II are the roll acceleration data from the MK. The unit of measurement is unknown as well.

Fig. 4 shows the linear line fitting with the measured data. According to the equation 7, the $k = 603.44 \text{ units}/g$ can be computed for the roll acceleration.

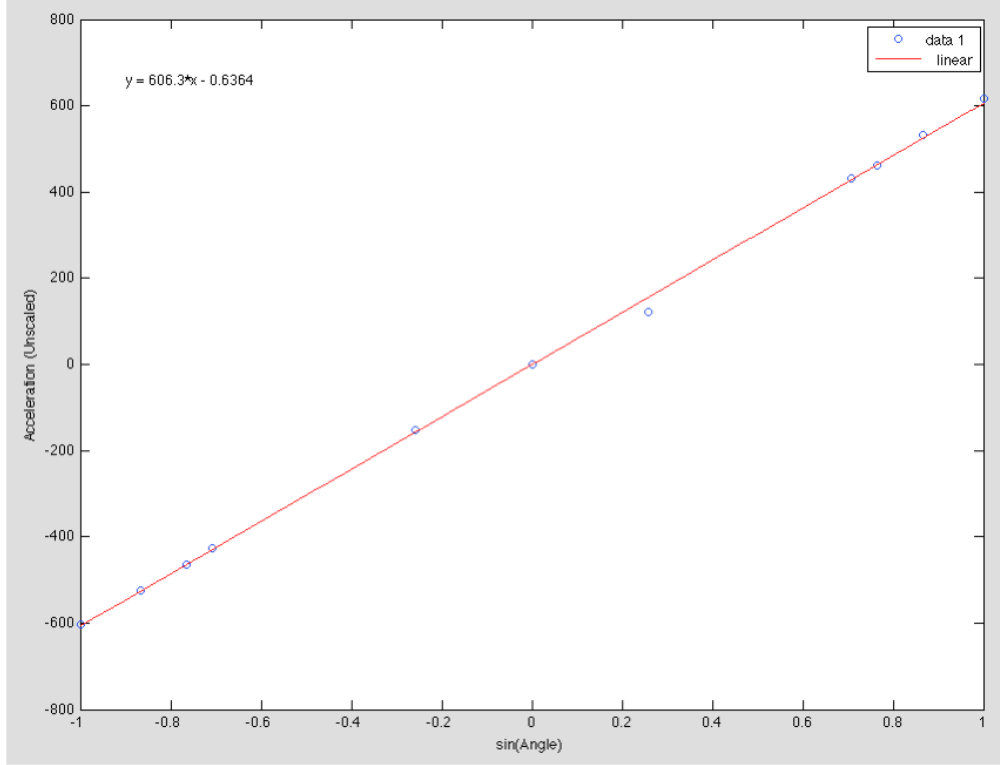


FIG. 3: MK pitch acceleration data versus true pitch angle.

Roll	-90°	-60°	-50°	-45°	-15°	0°	15°	45°	50°	60°	90°
1st	612	522	458	436	162	0	-167	-430	-462	-522	-587
2nd	611	521	456	443	161	0	-162	-432	-463	-515	-588
3rd	613	523	457	439	160	0	-165	-431	-463	-517	-588
Mean	612	522	457	439.3	161	0	-164.6	-431	-462.6	-518	-587.6

TABLE II: MK roll acceleration versus true roll angle measurement ruled by right hand

c. Z acceleration The drifting problem of raw ACCZ ADC measurement was found when vibration came from four rotors and it was thought that error accumulated when analog data was converted into digital. Hence the preprocessed MK default ACCZ value is exploited to estimate the z-velocity. The MK provides vibration robust filtered data but has an issue that it doesn't know what the unit is. In order to use this acceleration data

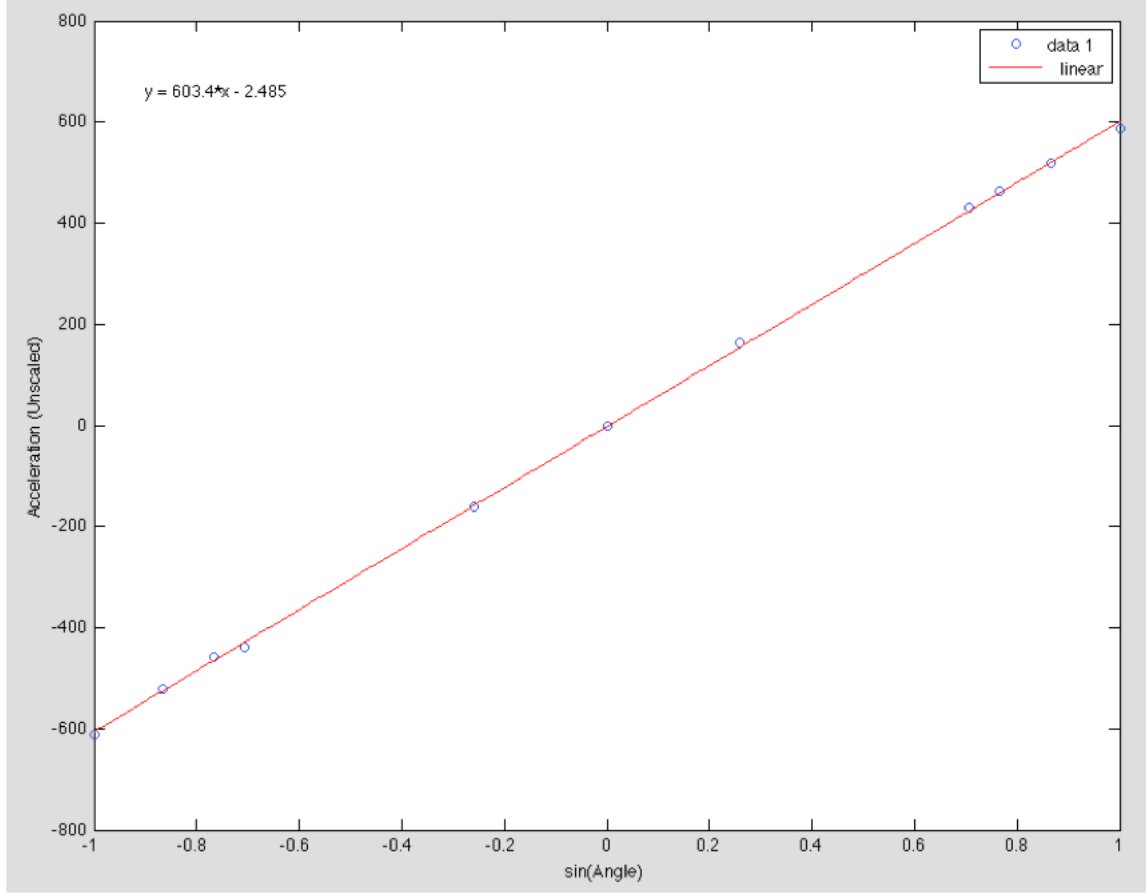


FIG. 4: MK AccRoll acceleration versus true roll angle.

for the complementary filter, the unit of data should be addressed. An experiment was conducted with a XSENS sensor. We put a XSENS on the quadrotor and logged XSENS and MK ACCZ data concurrently at the same sample rate(20 Hz), then matched the two data manually. Figure 5 shows the result.

$$ACCZ_{xsens}(t)[m/s^2] = \frac{ACCZ_{miko}(t)}{15.5} + 9.8 \quad (8)$$

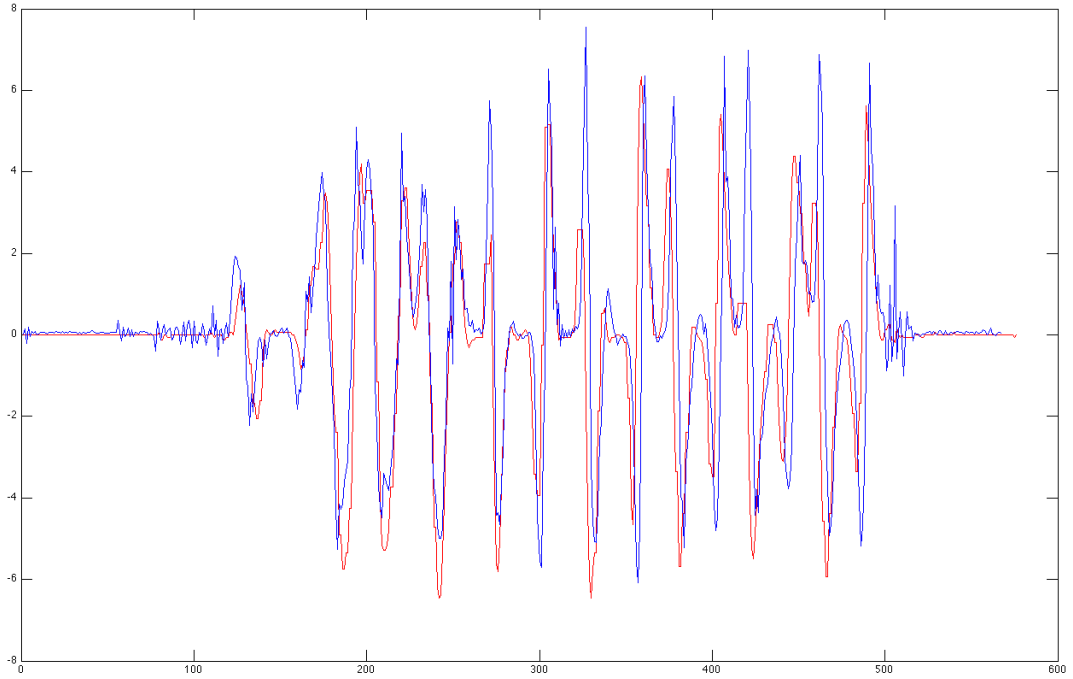


FIG. 5:

E. SI units and log message protocol

1. *SI units*

All units are used in the system following the SI units. All angle measurements are represented in **Radian** and **Metre** as a unit of all distance and angle measurements and **Second** is a unit of time. $\mathbf{m/s^2}$ is a unit of all acceleration.

2. *log message protocol*

There are two log messages. One is logging attitude of the quadrotor such as pitch angle and acceleration along x axis. Another measures data using the laser range finder like position, velocity and estimation of velocity. The reason why we have two log messages is because of different sampling rates of the laser range finder and the MK quadrotor. Position data based on the laser range finder comes into every $100ms$ and attitude of the quadrotor

Order	Notation	Description	Unit
1	g-W_Vel.x	World velocity along x axis.	m/s
2	g-B_Vel.y	Body velocity along x axis.	m/s
3	g-B_esti_Vel.x	Body estimated velocity along x axis.	m/s
4	g-W_Vel.y	World velocity along y axis.	m/s
5	g-B_Vel.y	Body velocity along y axis.	m/s
6	g-B_esti_Vel.y	Body estimated velocity along y axis.	m/s
7	g-CurrentPosition.x	current x position.	m
8	g-CurrentPosition.y	current y position.	m
9	g-CurrentPosition.theta	current angle.	radian
10	index	Counter increasing +1 every 100ms	number

TABLE III: 100ms loop log message format

is measured every 50ms.

a. 100ms sampling time TABLE III shows the 100ms sampling time log message protocol.

Order	Notation	Description	Unit
1	AnglePitch	Pitch angle	radian
2	AngleRoll	Roll angle	radian
3	AngleYaw	Yaw angle	radian
4	AccX	X acceleration with respect to the body frame	m/s^2
5	AccY	Y acceleration with respect to the body frame	m/s^2
6	AccZ	Z acceleration with respect to the body frame	m/s^2
7	ControlPitch	Pitch angle commanded to the quadrotor (-128 ~ 128)	unknown
8	ControlRoll	Roll angle commanded to the quadrotor (-128 ~ 128)	unknown
9	ControlYaw	Yaw angle commanded to the quadrotor (-128 ~ 128)	unknown
10	StickPitch	Transmitter pitch stick value (-128 ~ 128)	unknown
11	StickRoll	Transmitter roll stick value (-128 ~ 128)	unknown
12	StickYaw	Transmitter yaw stick value (-128 ~ 128)	unknown
13	StickThrust	Transmitter thrust stick value (0 ~ 255)	unknown
14	index	Counter increasing +1 every 50ms	number

TABLE IV: 50ms loop log message format

b. 50ms sampling time TABLE IV shows the 50ms sampling time log message protocol.

F. Complex dynamics of the MK quadrotor

In this section, dynamics of the MK quadrotor are presented.

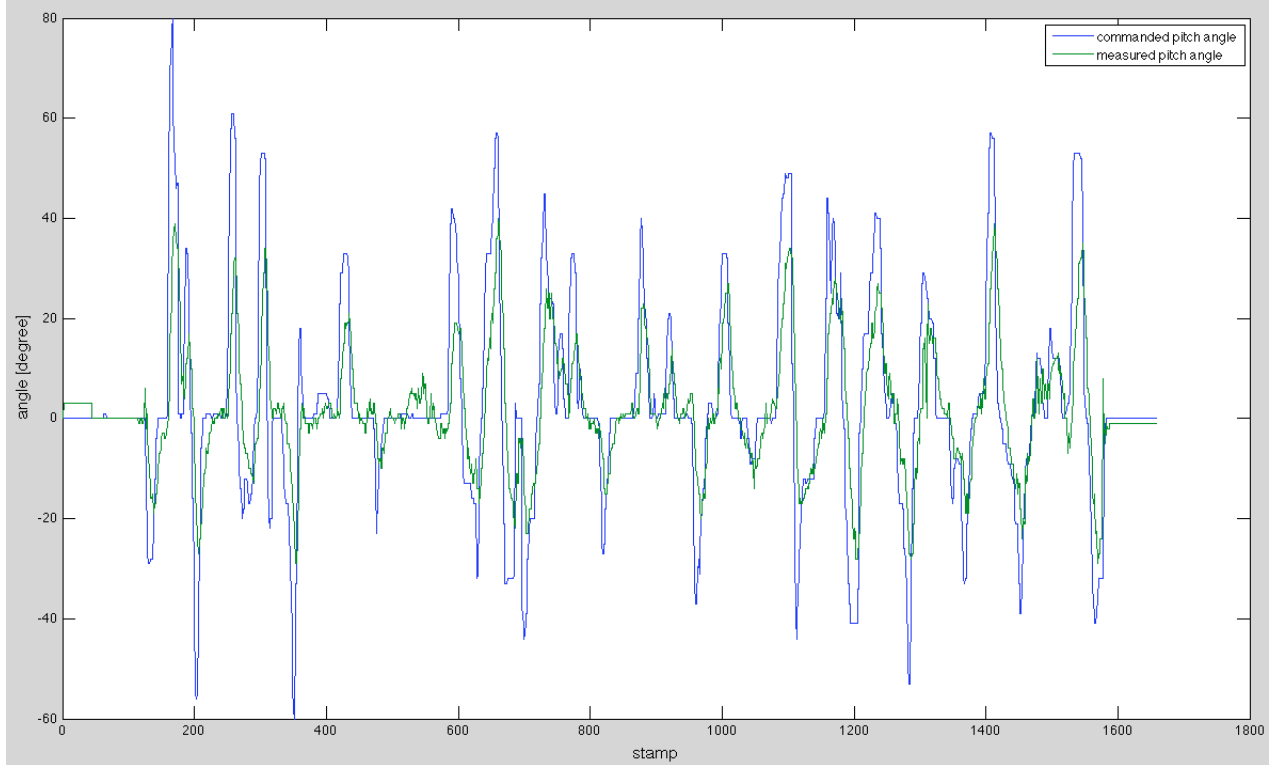


FIG. 6: Measured angle versus commanded angle

The lag can be resolved by looking at the vehicle velocity, in the vehicle frame, and correlating that with the pitch angle. Taking the cross correlation, Fig. 8 shows a lag of approximately 4 time steps which implies that the MK responses are $200ms$ later.

G. System latency

In order to find out the system latency between the Gumstix and the ground station, the network time protocol (NTP) server is exploited. NTP allows the setting up of two systems with less than $1ms$ time error. Fig. 9 shows synchronised systems and delay. After synchronisation, time duration was measured using ROS time stamp function. This function provides μs accuracy and it is sufficient to measure the time period.

Fig. 10 shows $100ms$ time delay of the laser range finder. Fig. 11 also shows $5ms$ delay of the ICP scan matcher. The WIFI latency can be determined by subtraction of

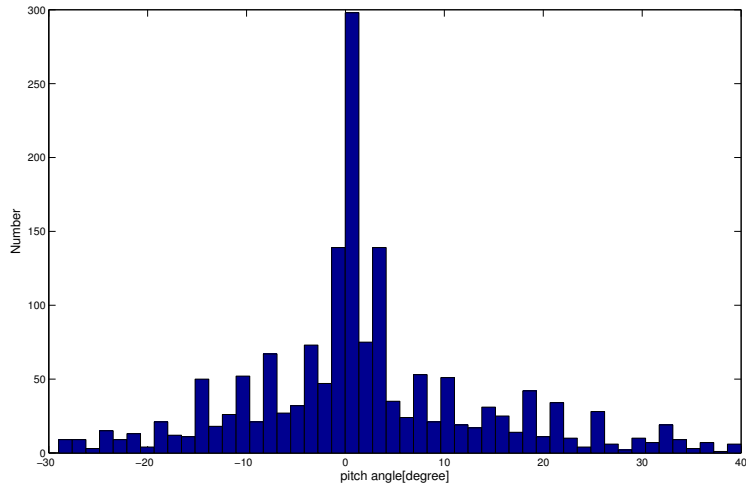


FIG. 7: Pitch angle histogram

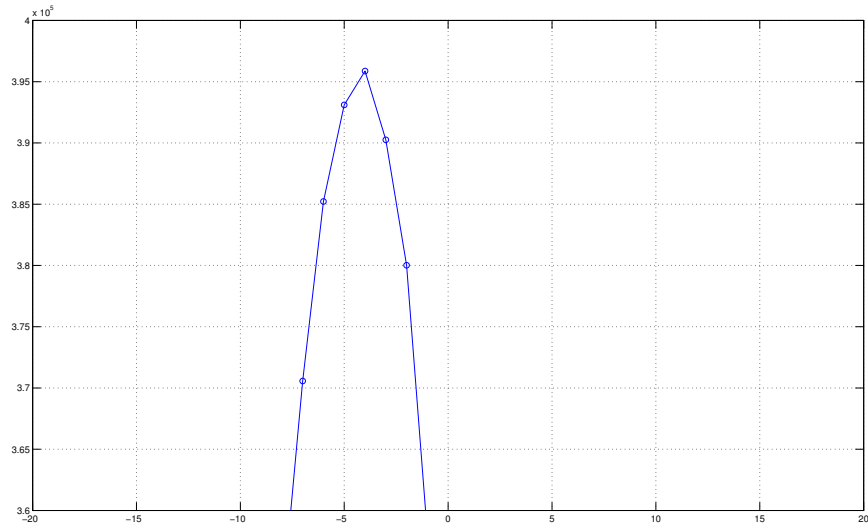


FIG. 8: Cross correlation

Current Time – Received Time. The WIFI latency is in the order of $7ms$.

In summary, figure 12 shows the total system latency in the system. As shown in the Fig. 8, the MK has about $200ms$ natural response time and WIFI, laser range finder and scan matcher have $167ms$ delay.

Desktop Time

```

enddl22@BEE-PG-46634:/opt/ros/cturtle/stacks/ccny-ros-pkg/scan_tools/canonical_s
can_matcher$ ntpq -p
      remote           refid      st t when poll reach  delay  offset jitter
=====
*LOCAL(0)          .LOCL.         5 l  57  64  377  0.000  0.000  0.001
enddl22@BEE-PG-46634:/opt/ros/cturtle/stacks/ccny-ros-pkg/scan_tools/canonical_s
can_matcher$

```

Gumstix Time, 1.4ms delay and -1.3ms offset.

```

      remote           refid      st t when poll reach  delay  offset jitter
=====
*BEE-PG-46634     LOCAL(0)         6 u  15  64  37  1.400  -1.368  5.944
224.0.1.1        .MCST.          16 u   -  64   0  0.000  0.000  0.031
enddl22@overo:~$

```

FIG. 9: Time synchronization using NTP server

```

[ INFO] [1298449895.438720160]: Stamps=1298449895.443614 seq=1225
[ INFO] [1298449895.540338157]: Stamps=1298449895.545232 seq=1226
[ INFO] [1298449895.641559328]: Stamps=1298449895.639066 seq=1227
[ INFO] [1298449895.735576580]: Stamps=1298449895.740471 seq=1228
[ INFO] [1298449895.837164052]: Stamps=1298449895.842089 seq=1229
[ INFO] [1298449895.938720998]: Stamps=1298449895.943645 seq=1230
[ INFO] [1298449896.040033745]: Stamps=1298449896.037449 seq=1231
[ INFO] [1298449896.133989947]: Stamps=1298449896.138914 seq=1232
[ INFO] [1298449896.235607946]: Stamps=1298449896.240532 seq=1233
[ INFO] [1298449896.337164894]: Stamps=1298449896.342089 seq=1234
[ INFO] [1298449896.438508167]: Stamps=1298449896.435862 seq=1235
^C[hokuyo-1] killing on exit
[ INFO] [1298449896.532616996]: Stamps=1298449896.537511 seq=1236
[ INFO] [1298449896.634204469]: Stamps=1298449896.639068 seq=1237

```

100ms delay

Stop streaming

1

FIG. 10: Laser time delay

```

[ INFO] [1298449896.037589707]: Latency is =0.000088 (sec) seq=1231
[ INFO] [1298449896.040960135]: publish Pose time=1298449896.040926
[ INFO] [1298449896.041064130]: dur: 3.301 ms ave: 3.368 ms, 1
[ INFO] [1298449896.131483510]: Latency is =-0.007491 (sec) seq=1232
[ INFO] [1298449896.134382413]: publish Pose time=1298449896.134351
[ INFO] [1298449896.134519430]: dur: 2.914 ms ave: 3.368 ms, 1
[ INFO] [1298449896.232897482]: Latency is =-0.007689 (sec) seq=1233
[ INFO] [1298449896.235949993]: publish Pose time=1298449896.235921
[ INFO] [1298449896.236050124]: dur: 3.030 ms ave: 3.367 ms, 1
[ INFO] [1298449896.334351894]: Latency is =-0.007790 (sec) seq=1234
[ INFO] [1298449896.338444963]: publish Pose time=1298449896.338395
[ INFO] [1298449896.338582200]: dur: 4.113 ms ave: 3.368 ms, 1
[ INFO] [1298449896.435851942]: Latency is =-0.000087 (sec) seq=1235
[ INFO] [1298449896.439757568]: publish Pose time=1298449896.439726
[ INFO] [1298449896.439862807]: dur: 3.869 ms ave: 3.368 ms, 1
[ INFO] [1298449896.531759971]: Latency is =-0.005812 (sec) seq=1236
[ INFO] [1298449896.535337901]: publish Pose time=1298449896.535296
[ INFO] [1298449896.535464662]: dur: 3.554 ms ave: 3.369 ms, 1

```

2

FIG. 11: ICP time delay and wifi latency

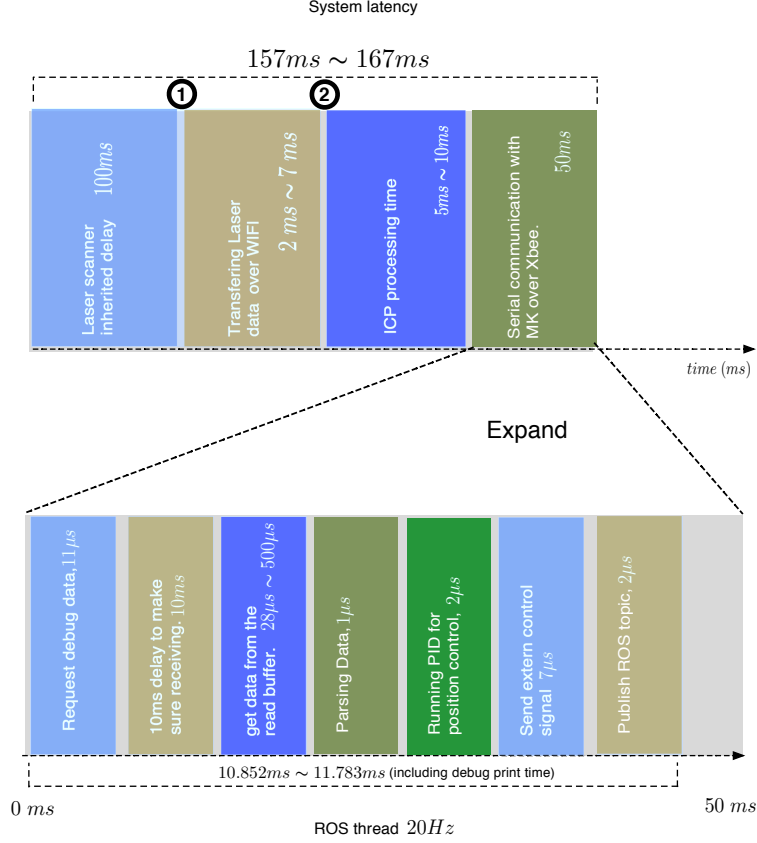


FIG. 12: The total system latency

H. Velocity estimation

It is necessary to use a velocity estimator because of the complex dynamics and latency of the system. A complementary filter is exploited and this requires accelerations of each axis in order to estimate velocities.

1. X axis acceleration

the velocity in body frame. The acceleration along the x axis is

$$a_x = {}^B\ddot{x} \cos \theta - g \sin \theta \quad (9)$$

$${}^B\ddot{x} = \frac{a_x + g \sin \theta}{\cos \theta} \quad (10)$$

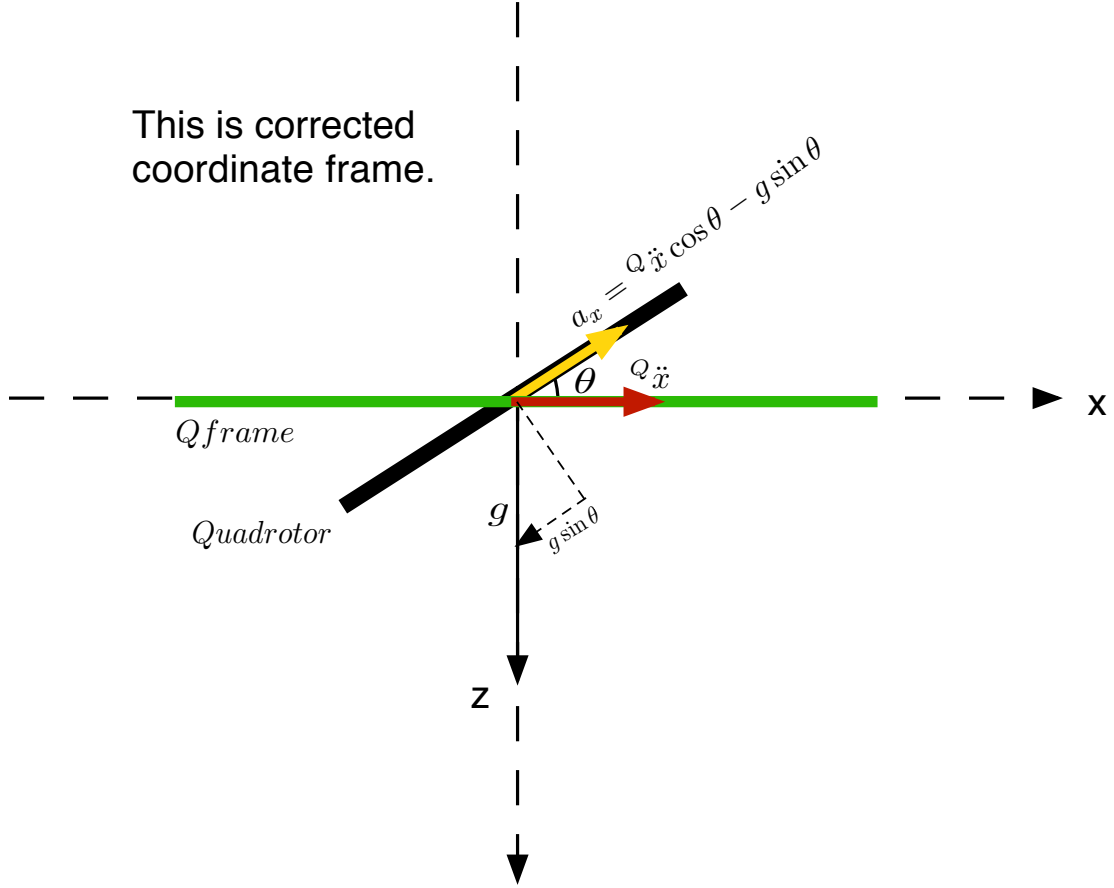


FIG. 13: X axis acceleration

2. Y axis acceleration

The acceleration along the y axis is

$$a_y = {}^B\ddot{y} \cos \phi + g \sin \phi \quad (11)$$

$${}^B\ddot{y} = \frac{a_y - g \sin \phi}{\cos \phi} \quad (12)$$

${}^w x$, ${}^w y$, ${}^w v_x$ and ${}^w v_y$ refer to the position and velocity in world frame respectively. ψ is measured orientation in world frame. ${}^b v_x$ and ${}^b v_y$.

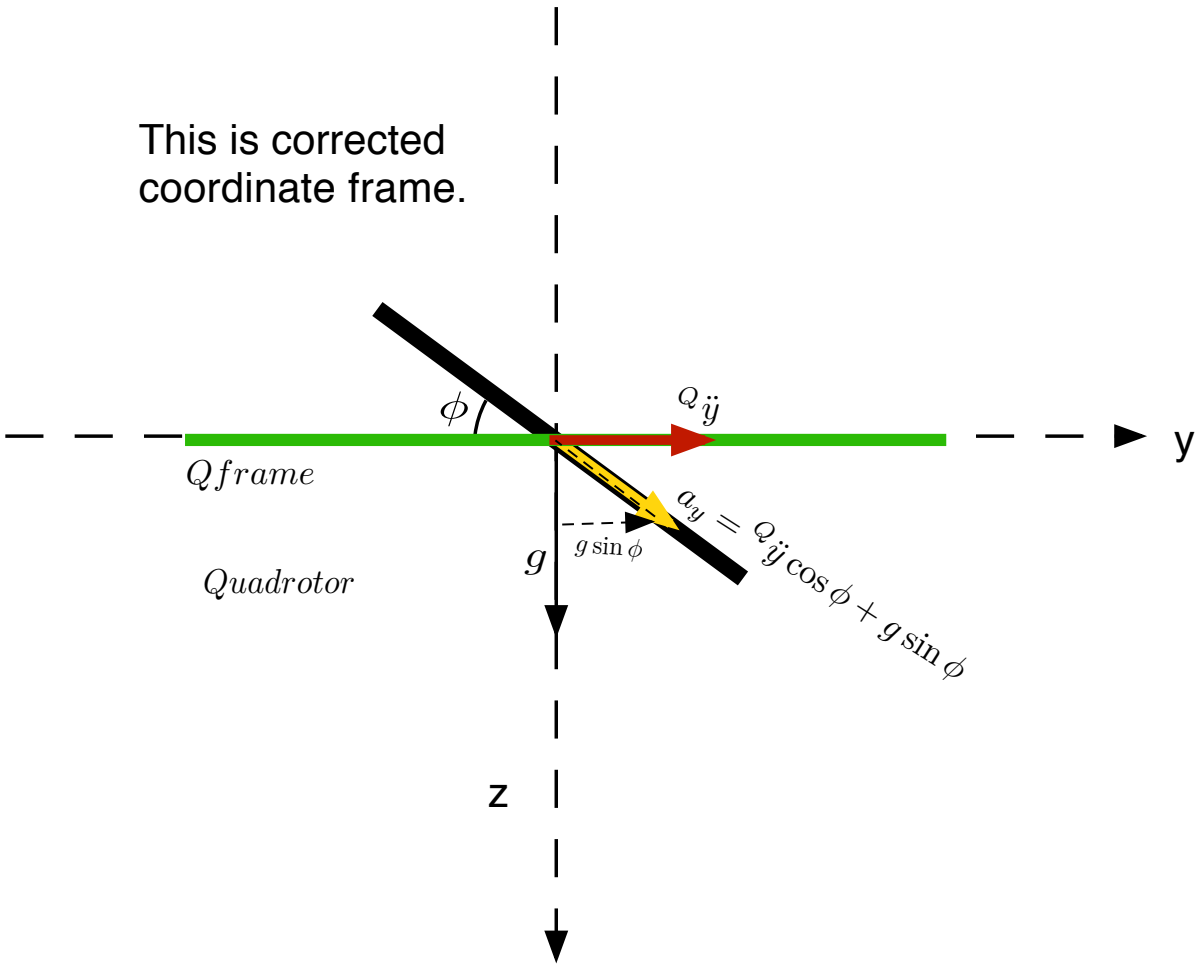


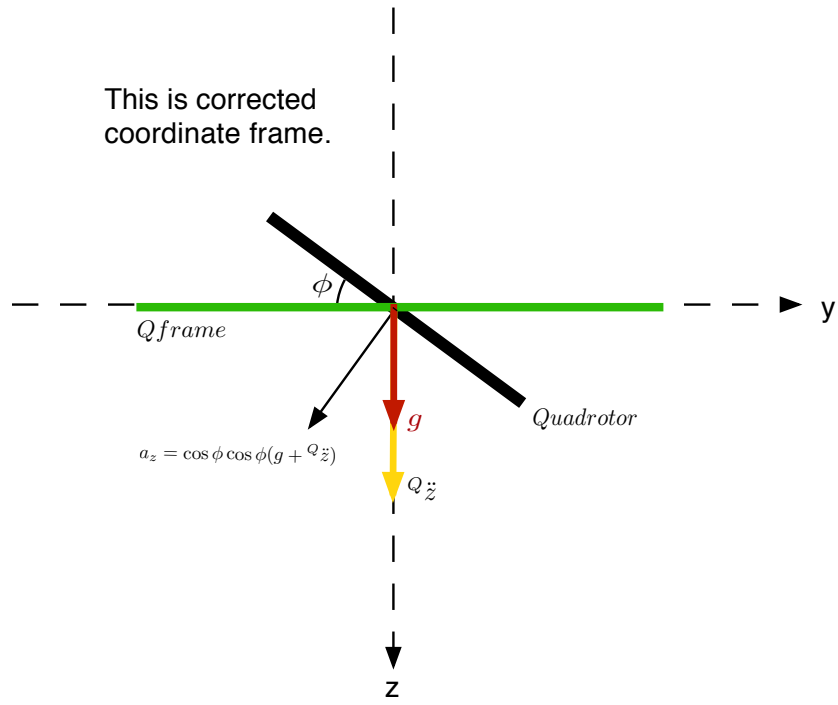
FIG. 14: Y axis acceleration

3. Z axis acceleration

The acceleration along the z axis is

$$a_z = \cos \phi \cos \theta (g + Q \ddot{z}) \tag{13}$$

$$Q \ddot{z} = \frac{a_z}{\cos \phi \cos \theta} - g \tag{14}$$



a. A complementary filter

$$\hat{v}_x(t+1) = \hat{v}_x(t) + T (k ({}^B v_x - \hat{v}_x(t)) + Q \ddot{x}) \quad (15)$$

$$\hat{v}_y(t+1) = \hat{v}_y(t) + T (k ({}^B v_y - \hat{v}_y(t)) + Q \ddot{y}) \quad (16)$$

$$\hat{v}_z(t+1) = \hat{v}_z(t) + T (k ({}^B v_z - \hat{v}_z(t)) + Q \ddot{z}) \quad (17)$$

where T is the sample interval, and k is the filter gain.

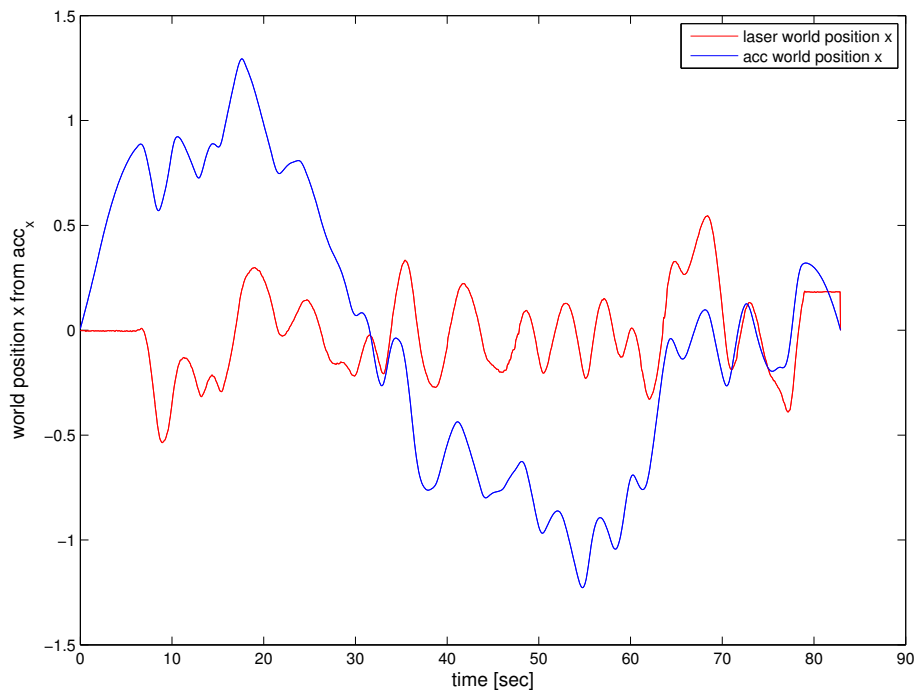


FIG. 16: X position in world frame for laser-based localizer

Fig. 16 is the one sample predicted position using Equation 18. We assume that the quadrotor is hovering and the velocity of it is almost constant.

$$\hat{x}(t+1) = x(t) + v(t) \cdot T \quad (18)$$

$$= x(t) + \frac{x(t) - x(t-1)}{T} \cdot T \quad (19)$$

$$= 2x(t) - x(t-1) \quad (20)$$

Fig. 17 shows the velocity in body frame calculated derivative of the x position and Equation 4.

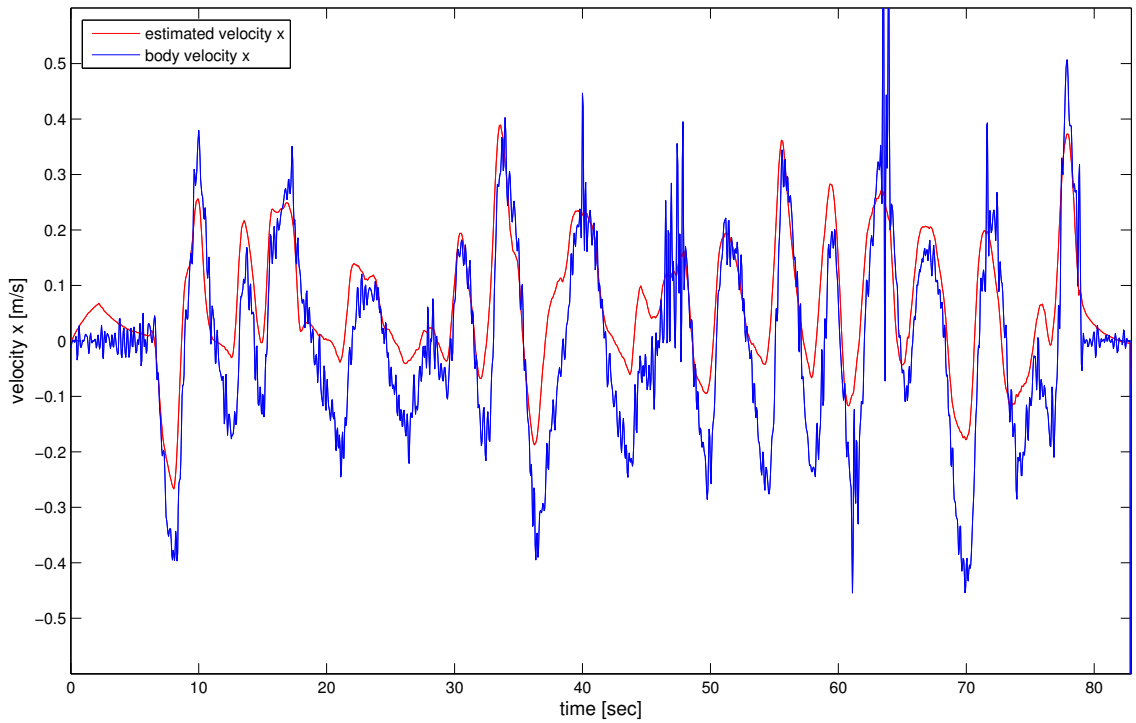


FIG. 17: x velocity versus estimated x velocity in body frame

Fig. 17 shows the estimated velocity in body frame using Equation 15 and 16.

Fig. 18 plots the command data which generated by Equation 21.

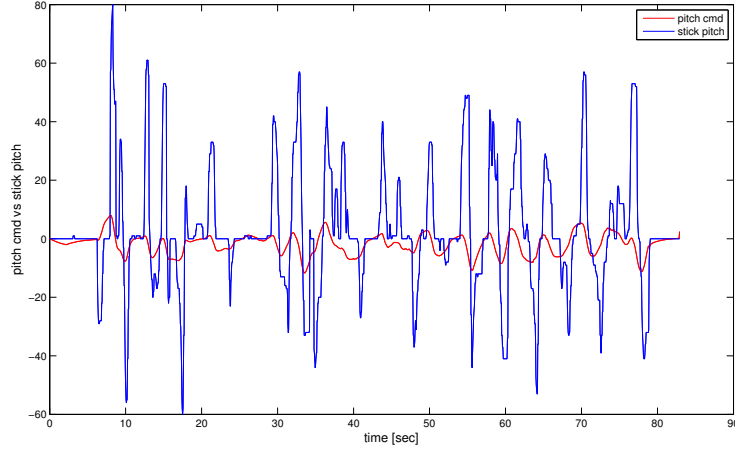


FIG. 18: Pitch command generated with P velocity controller

$${}^W\theta^*(t) = K_p({}^Wv_x^*(t) - {}^W\hat{v}_x(t)) + K_d\frac{d}{{}^Wv_x^*(t) - {}^W\hat{v}_x(t)} \quad (21)$$

$${}^W\phi^*(t) = K_p({}^Wv_y^*(t) - {}^W\hat{v}_y(t)) + K_d\frac{d}{{}^Wv_y^*(t) - {}^W\hat{v}_y(t)} \quad (22)$$

$${}^W\tau^*(t) = K_{p_{gas}}({}^Wv_z^*(t) - {}^W\hat{v}_z(t)) + K_{d_{gas}}\frac{d}{{}^Wv_z^*(t) - {}^W\hat{v}_z(t)} \quad (23)$$

In the Equation 21 we assume that ${}^Wv_x^*(t)$ and ${}^Wv_y^*(t)$ are zero to hovering.

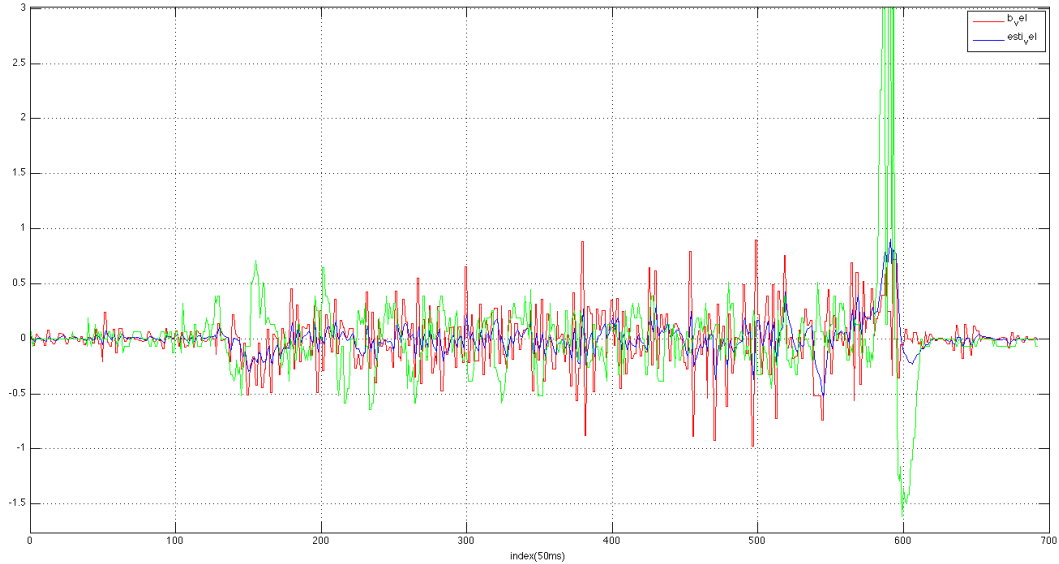


FIG. 19: This plot shows estimated velocity along z axis. Green, Red and Blue lines stand for ACCZ from MK, body velocity and estimated velocity. ACCZ is sampled at 20 Hz and estimated velocity is computed at the same rate. The body velocity is calculated based on laser range finder height data and has a sample rate of 10 Hz. Note that body velocity is smoothed.

I. ROS implementation

It is easily achieved to integrate systems with ROS. All messages come into the ROS core and are redistributed to nodes through the TCP/IP protocol. This feature allows implementation of the software packages as modules, ROS stacks or packages. Fig. 20 shows simple implementation based on the ROS. In this figure, dark gray boxes denotes the ROS nodes which act as an individual process. The canonical scan matcher receives laser range data and produces 2D positions using the ICP algorithm. It publishes $/pose2D$ topic every $100ms$ and the data structures are shown in TABLE V and TABLE VI. A Miko Serial node functions are as obtaining IMU data from the flight control board while a quadrotor is flying and publishing $/mikoImu$ topic every $50ms$. These two topics can be recorded to create a log file and be played using rosbag package. Finally, a complementary Filter node

Name	geometry_msgs/Pose2D		
Description	This expresses a position and orientation on a 2D manifold.		
Data type	definition	Unit	Description
float64	x	<i>m</i>	x position in world frame
float64	y	<i>m</i>	y position in world frame
float64	theta	<i>radian</i>	theta angle in world frame

TABLE V: /Pose2D topic data type

computes body and estimated velocity given position and IMU data with Equation 15 and 16. With this complementary filter, the position control of the quadrotor can be achieved. The demonstration footage can be found on the [Youtube](#).

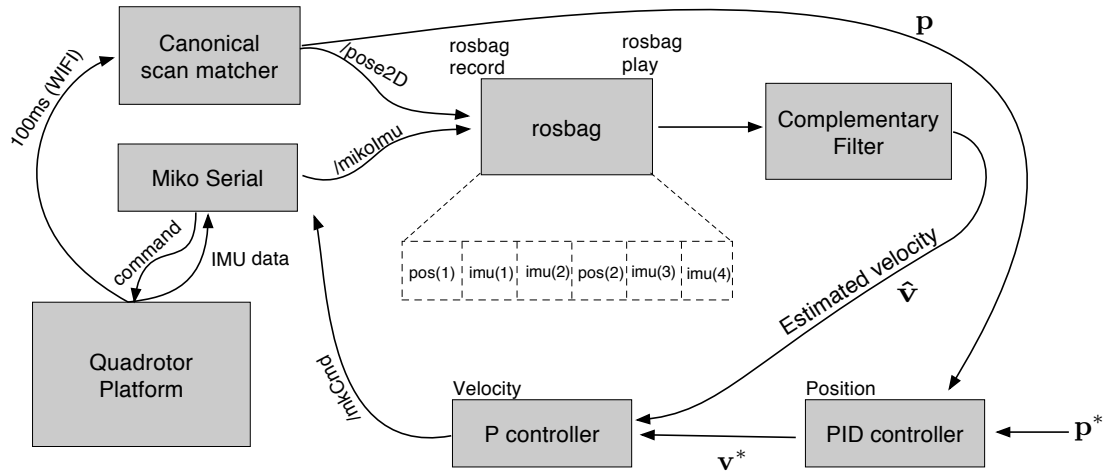


FIG. 20: ROS complementary filter implementation

J. Yaw control

Yaw control of the quadrotor is relatively easier than pitch, roll and height control. Gyro data is drifting overtime which implies the vehicle is going to change its heading. Therefore

Name	sensor_msgs/mikoImu		
Description	This expresses a attitude of a quadrotor.		
Data type	definition	Unit	Description
float64	pitchAngle	<i>radian</i>	pitch angle in body frame
float64	rollAngle	<i>radian</i>	roll angle in body frame
float64	yawAngle	<i>radian</i>	yaw angle in body frame
float64	AccX	m/s^2	Acceleration along x axis in body frame
float64	AccY	m/s^2	Acceleration along Y axis in body frame
float64	AccZ	m/s^2	Acceleration along Z axis in body frame

TABLE VI: /mikoImu topic data type

Name	sensor_msgs/mikoCmd		
Description	This expresses command input to the quadrotor.		
Data type	definition	Unit	Description
int32	pitch		pitch cmd -128 ~ 128
int32	roll		roll cmd -128 ~ 128
int32	yaw		yaw cmd -128 ~ 128
int32	throttle		throttle cmd 0 ~ 512

TABLE VII: /mikoCmd topic data type

we need to use the absolute measurement data which is less changed as time passes. Laser range data can provide the yaw angle with minimum error as its variance is smaller than a gyro sensor. A traditional PID controller is used to hold the position. The equation 24 shows this controller and figure 21 presents the output and yaw angle. In this figure, the pilot gives the artificial angle using the transmitter and the controller generates the output to keep the initial angle "0".

$$u(t) = K_p e(t) + K_i \int_0^t e(\tau) d\tau + K_d \frac{d}{dt} e(t) \quad (24)$$

where $e(t) = \psi^* - \psi$

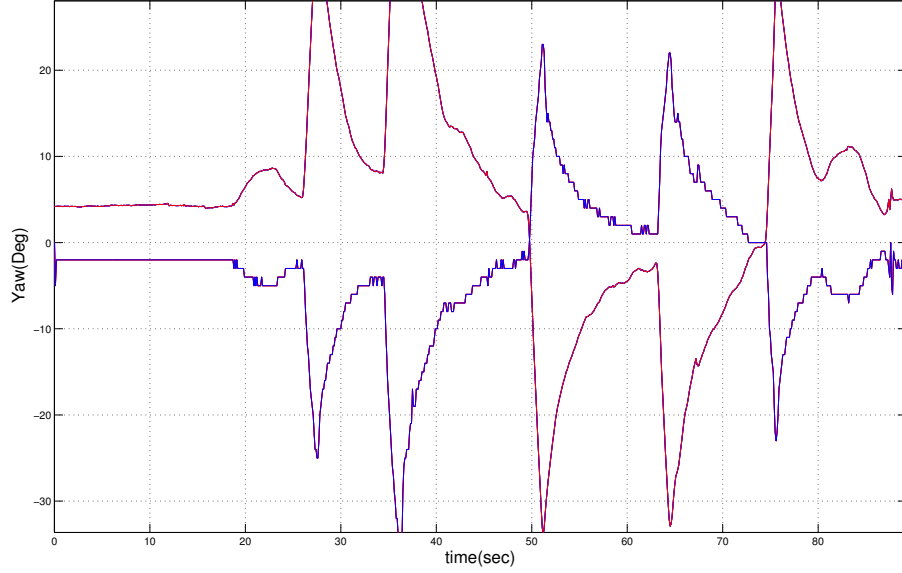


FIG. 21: Yaw angle and yaw command output using PID controller.

K. Altitude control

In order to implement the height controller, it is a compulsory requirement to make sure safety. Once the vehicle gets a wrong command such as putting negative sign on the *unsigned char* variable, it flies to the sky at a full speed. In fact, this can be a very frightening moment. To avoid this kind of accident, the MK limits the FC code to prevent the user from controlling the gas value if the control cmd value is bigger than the stick gas. To achieve the altitude control, the FC code requires modification by enabling the external control with the saturation function that limits the range from 0 to 130. This number is the threshold of the gas value which lets the vehicle fly with the current payload and is obtained empirically.

1. PID altitude control

$$u(t) = K_p e(t) + K_i \int_0^t e(\tau) d\tau + K_d \frac{d}{dt} e(t) \quad (25)$$

where $e(t) = z^* - z$ and z^* denotes the desired position along z axis and z is the current position. In addition, the height measurement is coupled with θ and ϕ . The projected estimation of the height can be determined as the following equation.

$$\hat{z} = \cos \theta \cos \phi z \quad (26)$$

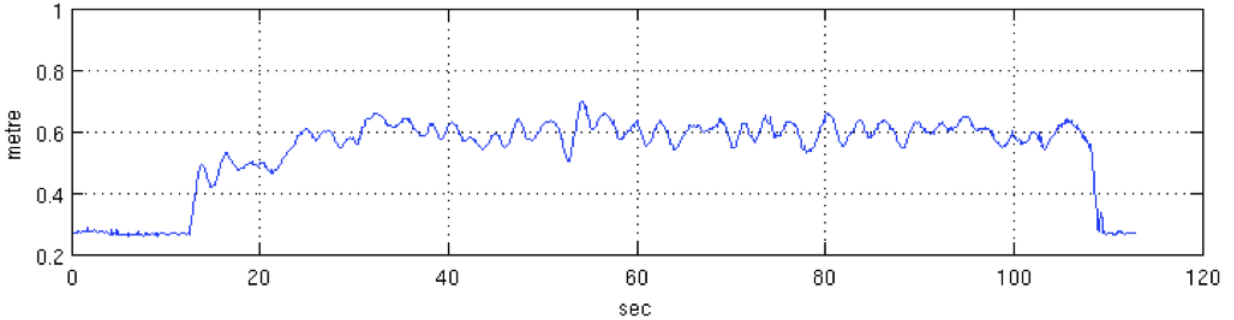


FIG. 22: Height measurement data using PID control with a goal at 0.6 metre. The input for the PID controller is the height measurement from laser hat and output is throttle control command. The MK uses **unsigned char** data type to control quadrotor range from ± 127 . Note that average height measurement is within ± 5 cm. Rarely does maximum error goes up up to ± 10 cm owing to ground effect and aerodynamics, but the quadrotor quickly converges into the goal.

L. Flight time calculation

Flight time is essential to the MAV research area. Many research platforms can only fly for up to 10 minutes or less. However, the MK platform is able to fly up to 41 minutes unofficially. The video demonstration can be found on [vimeo](#). Detailed information can be

found in the article of [MikroKopter wiki page](#). In order to estimate the flight time given payload, we need to know total weight of a vehicle. In our case, the quadrotor weight is around $\approx 1,040\text{g}$ including frames, laser range finder, Gumstix, XBee, laser hat and battery. Therefore 260g is the thrust per motor.

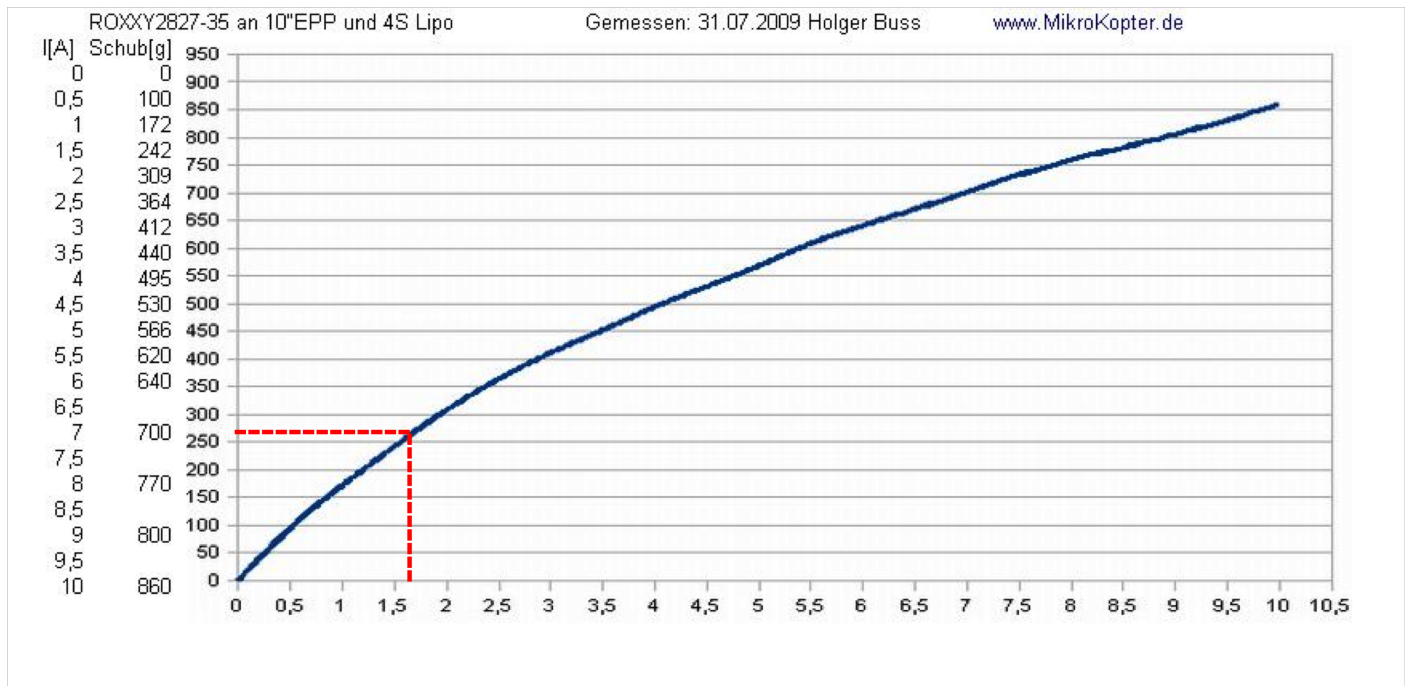


FIG. 23: The Ampere Versus payload characteristic of ROXXY2827-35 motor.

From figure 23, we could notice that a motor consumes around $\approx 1.7\text{A}$. This implies that there is a total current of $6.8\text{A} = 1.7 \times 4$.

$$t = \frac{B}{C} \quad (27)$$

Where t is the total flight time in units of hour, B and C are battery capacity and Total current respectively. A Lipo battery, 2.2Ah, 4 cells, was used and Figure 27 shows 0.323 hour = 19.4 minutes flight time. This flight time is an ideal value that specifies the absolute limit. These factors should be taken account.

- The thrust characteristic was measured with a 100% loaded LiPo. The thrust decreases slightly when the voltage drops in flight.

- Turbulence
- Losses due to regulations
- Other losses (e.g. in cables, etc.)

For these reasons, a scale factor, 0.9, was multiplied. This parameter is chosen empirically and should be changed as the battery efficiency goes down.

In conclusion, the estimated total flight time is **17.4 minutes** and this value also can be found in Figure 24. This graph is validated by comparison of our previous work as described in Figure 25

Moreover, extra power consumption electric parts are used such as a laser range finder, a Gumstix, a XBee module and a USB HUB. These parts also consume energy and reduce the total flight time. [The power consumption of the Gumstix](#) is order of 2.5W ~ 5W and the laser range finder spends 2.5W. Hence, the extra power consumption could be said to be less than 0.5A. Finally, from the calculation our quadrotor can fly up to **16.28 minutes**, $0.9 \times \frac{2.2}{6.8+0.5}$.

M. Battery discharge dynamics

We logged Lipo batteries, (3cell, 2200mAh), to compensate the trust offset. Interestingly, each battery showed a different discharge curve. (see Figure 26).

N. Platform price comparison.

The advantage of the MK is a competitive price. As described in Table VIII, it is a lot cheaper than a similar level of research platform. Although MK Basicset is needed to put all parts together before flight, there is detailed documents on the MK web. In addition, it is feasible to modify the platform for user's demands. The pelican from Asecnding Technology is **6.41** times more expensive than MK quadrotor.

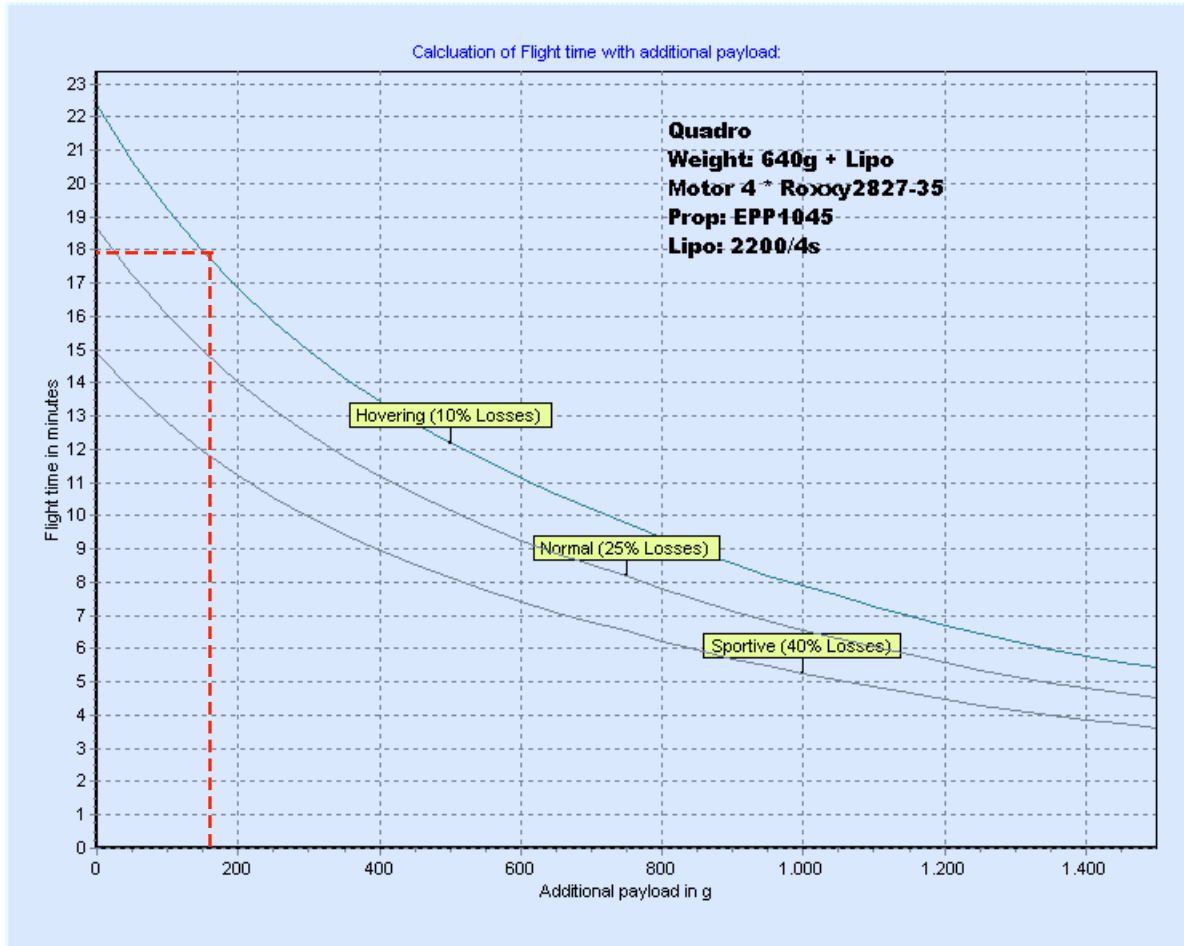


FIG. 24: Flight time Versus payload characteristic graph. Total weight of the vehicle is 1,040g and this graph shows the flight time with 640g+238g (battery) payload. Therefore, the payload is 162g. In addition, the hovering graph is appropriate for the indoor application.

O. Precision comparison

In this section, a variety of accuracy and precisions of state estimations are presented when a quadrotor performs hovering or following given trajectory. As MAVs have fast dynamics, filtering techniques such as complementary filter and Kalman Filter are often used to estimate the state of the vehicle. Table IX shows a summary of precision from 5 different research groups.[2][5][1][3][4]

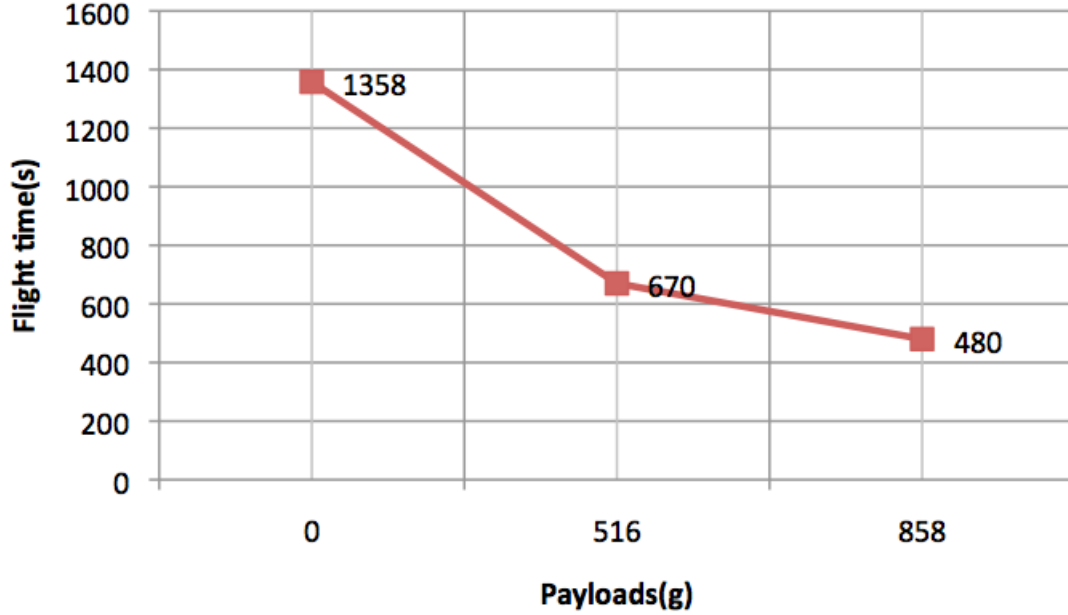


FIG. 25: Payload Versus Flight time table. This table was measured by us.

	Mikrokopter	Price(USD)	Asecnding Tech	Price(USD)
platform	MK Basicset	987.46	Pelican	7435.09
Transmitter	6CH	169.99	7CH	499.49
Receiver	7 CH	79.99		
Total		1237.44		7934.58
Ratio				6.41

TABLE VIII: This table shows prices comparison between the MK Quadrotor set and the similar level platform of Ascending technology, Pelican. These prices come from [MikroKopter](#) , [HobbyKing](#) and [Ascending Tech](#).

P. Ground truth and estimation.

In this section, we compare ground truth from the VICON system to our dynamic state estimation. We estimate position $\hat{x}, \hat{y}, \hat{z}$ and velocity \hat{V}_x, \hat{V}_y . in addition, The MK estimates pitch(θ), roll(ϕ) and yaw(ψ) angles.

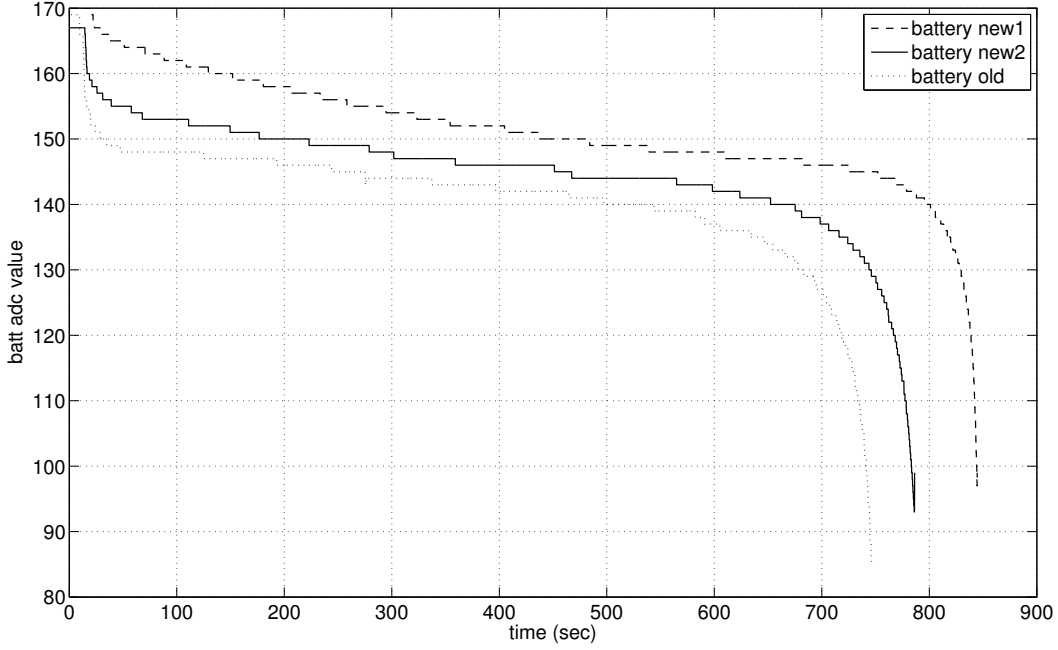


FIG. 26: Lipo battery discharge curves. X axis denotes time and y axis is a battery ADC reading value.

1. VICON coordinate system and experiment setup

Figure 28 shows VICON coordinate and experiment configuration. Since the maximum range of the laser range finder attached to the quadrotor is 4m, we need to put structures within the 4m range. VICON system tracks infrared beam reflected by each makers and provides position and orientation of the makers. Figure 29 shows the place where makers on the quadrotor are attached. By computing error of Euclidean distance between two markers, Equation 28 VICON system shows $\pm 5\text{mm}$ position error. We could find the distance error increased after taking off because of frame vibration.

$$e = e_{initial} - \sqrt{(x_{maker1} - x_{maker2})^2 + (y_{maker1} - y_{maker2})^2 + (z_{maker1} - z_{maker2})^2} \quad (28)$$

where $e_{initial}$ denotes the very first distance between markers.

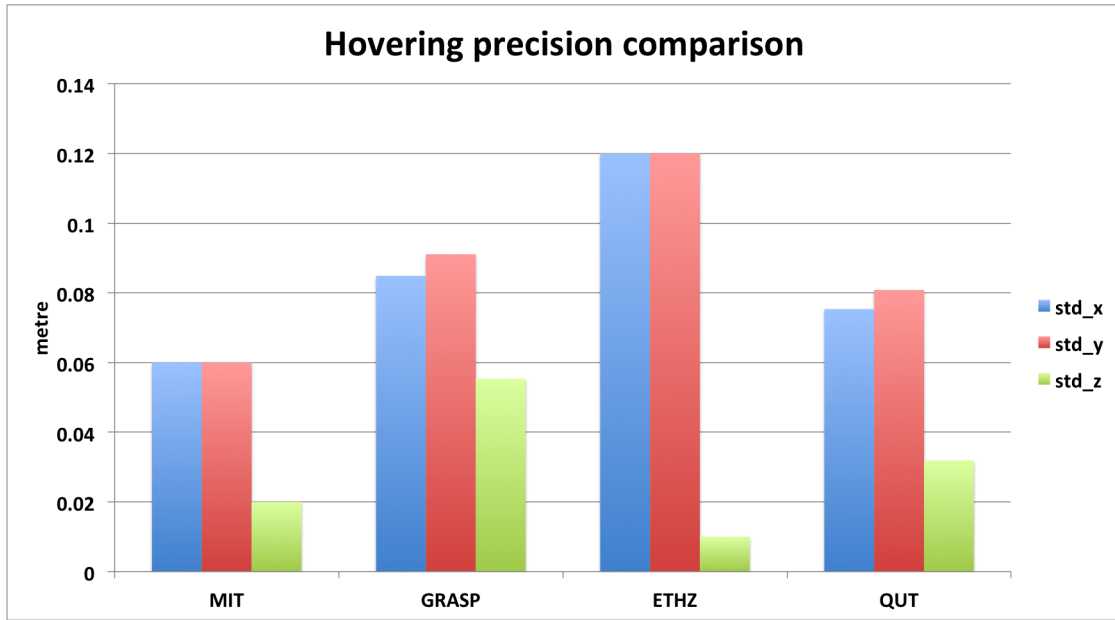


FIG. 27: Precision comparison of state-of-the-art platforms.

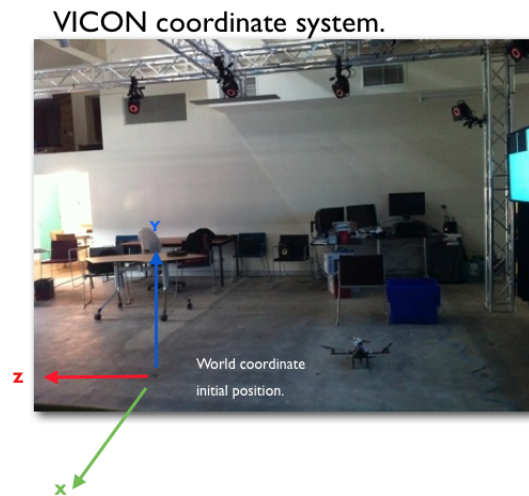


FIG. 28: This photo shows the VICON system coordinate and setup. This system is equipped with 14 cameras to track markers and provides position, normal and orthogonal.

A "x" mark on the ground is the initial position of VICON system. The coordinate transformation is required from VICON coordinate to MK coordinate as described in 2.



FIG. 29: Two makers are attached in order to calculate position error of VICON system.

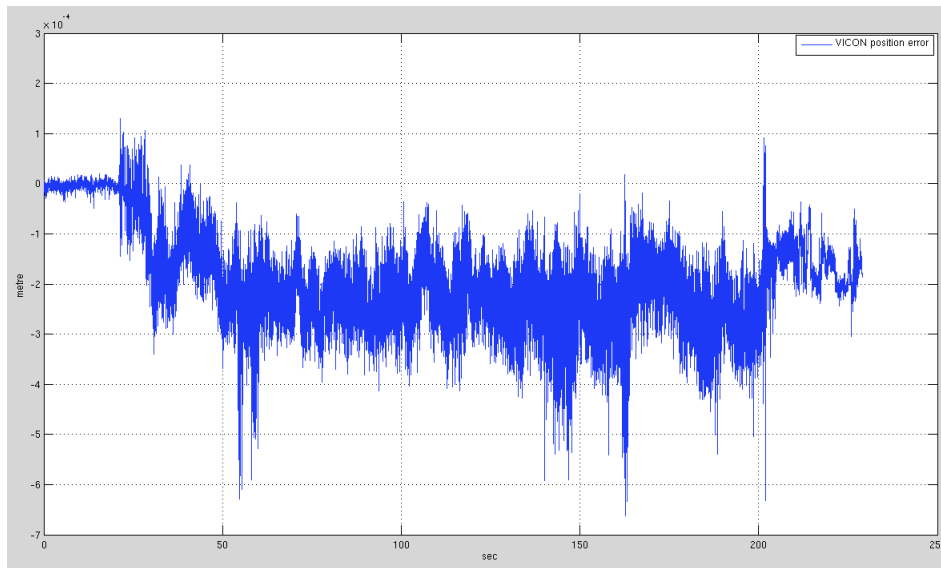


FIG. 30: Position error between two markers. Note that the quadrotor starts taking off and increasing position error due to frame vibration around 22sec. Mean is 0.0002 metre.

TABLE IX:

University	MIT(RANGE)[2]	GRASP Lab.[5]	ETHZ(ASL)[1]
Year	2010	2011	2011
Precision	Hovering	Hovering	Hovering
(metre)	RMS_X= 0.06	Std_X= 0.0849	RMS_X=0.12
(metre)	RMS_Y= 0.06	Std_Y= 0.0911	RMS_Y=0.12
(metre)	RMS_Z= 0.02	Std_Z= 0.0554	RMS_Z=0.01
	Trajectory following	Trajectory following	
(metre)	RMS_X=0.07	Std_X=0.0247	
(metre)	RMS_Y=0.07	Std_Y=0.0323	
(metre)		Std.Z=0.007	
Platform	Pelican	Pelican	Pelican
Sensor	Laser 40Hz	Laser 40Hz	1000Hz IMU
			10Hz mono Vision
			Fusion
University	Freiburg[3]	Oxford(Chris Kemp) [4]	QUT
Year	2009	2006	2011
Precision			Hovering
(metre)			Std_X=0.075368
(metre)			Std_Y=0.080849
(metre)	Error_Z=±0.1	Error_Z=±0.1	Std_Z=0.031913

a. Position estimation Figure 31 and Figure 32 show ground truth and position, velocity estimation.

II. REFERENCES

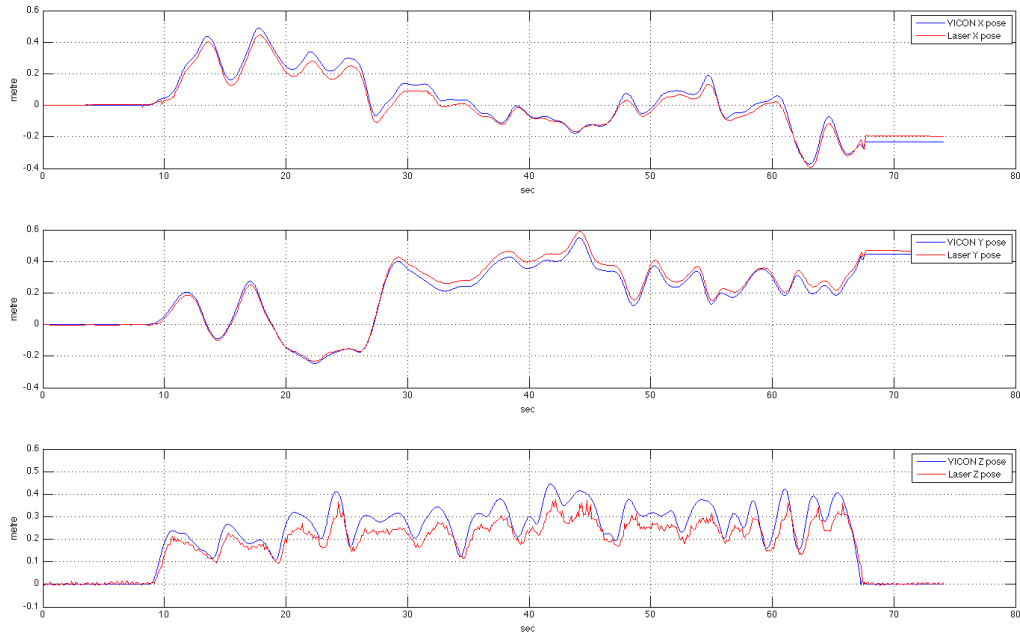


FIG. 31: Blue is the ground truth and red is the laser position estimation. The x-axis is time in second, the y-axis is position in unit of metre.

-
- [1] Markus Achtelik, Michael Achtelik, Stephan Weiss, and Roland Siegwar. Onboard imu and monocular vision based control for mavs in unknown in- and outdoor environments. In ICRA2011, 2011.
 - [2] A. Bachrach, A. de Winter, Ruijie He, G. Hemann, S. Prentice, and N. Roy. RANGE - robust autonomous navigation in GPS-denied environments. In Robotics and Automation (ICRA), 2010 IEEE International Conference on, pages 1096 –1097. MIT, may 2010.
 - [3] S. Grzonka, G. Grisetti, and W. Burgard. Towards a navigation system for autonomous indoor flying. In Robotics and Automation, 2009. ICRA '09. IEEE International Conference on, pages 2878 –2883, may 2009.
 - [4] Christopher Kemp. Visual Control of a Miniature Quad-Rotor Helicopter. PhD thesis, Univer-

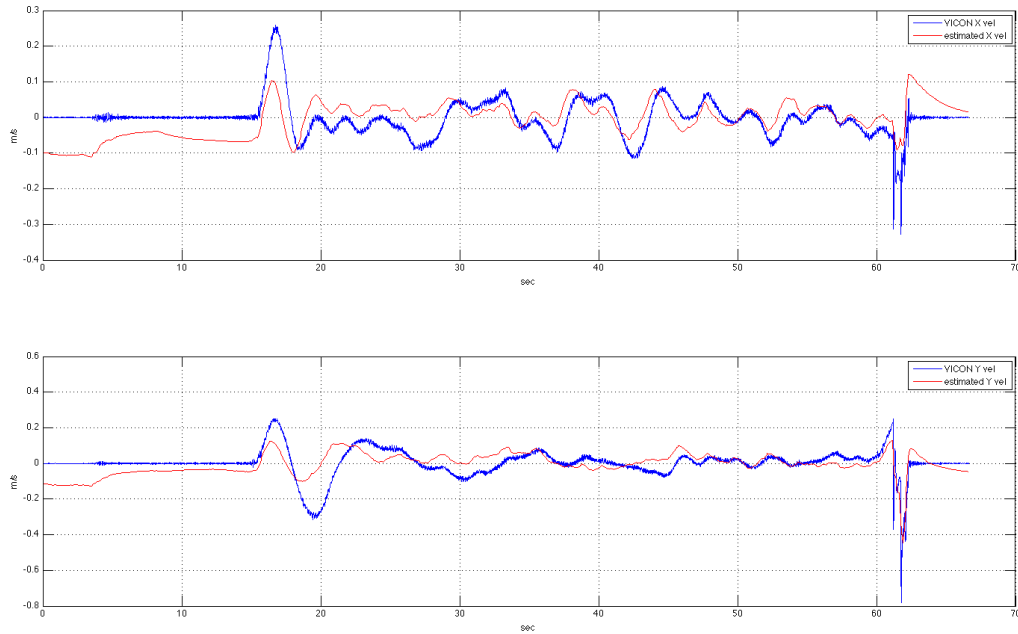


FIG. 32: Blue is the ground truth and red is the velocity estimation from complementary filter. The x-axis is time in second, the y-axis is velocity in unit of m/s .

sity of Cambridge, 2006.

- [5] Shaojie Shen, Nathan Michael, and Vijay Kumar. Autonomous multi-floor indoor navigation with a computationally constrained mav. In 2011 IEEE International Conference on Robotics and Automation, 2011.

Appendix A: Matlab implementation

To implement a complementary filter, a simulation was conducted with MATLAB. The data that was used for simulation was obtained by manual pilot. All data was converted into SI units, metres and radians. The follow is the MATLAB code.

```

1 clear all;
  data=importdata('data_Manual_Coordinate',' ',1);
3
  samp_time=0.05; % second/50ms sampling time
5 W_x=data.data(:,10)/1000; % unit=metre X position
  W_y=data.data(:,11)/1000; % unit=metre Y position

```

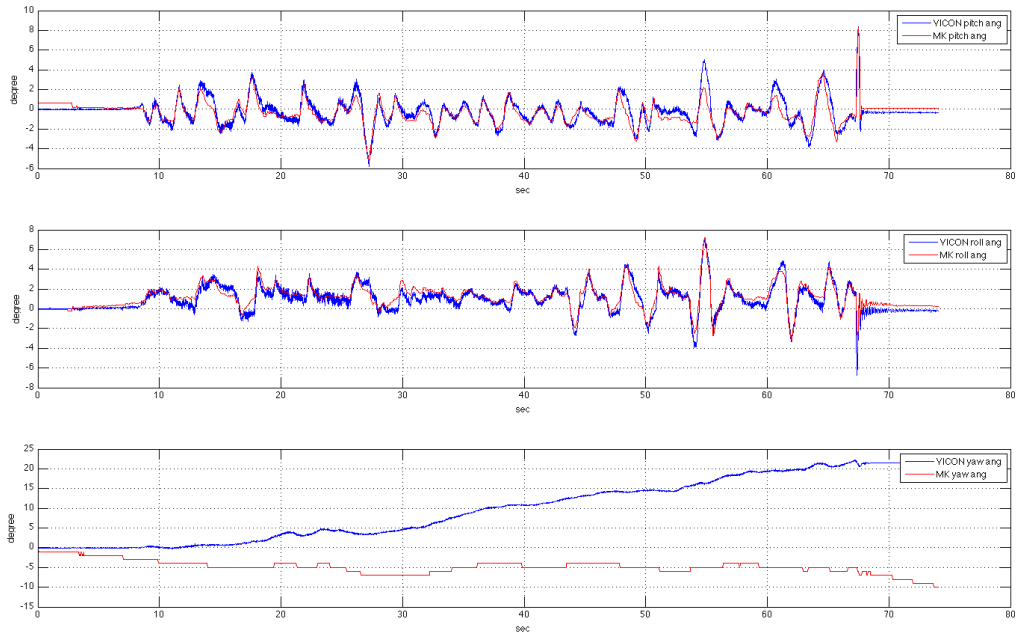


FIG. 33: Blue is ground truth and red is angle estimation by accumulating angular rates of gyro sensor. The x-axis is time in second, the y-axis is the angle in unit of degree. This data comes from the MK.

```

7 time=data.data(:,15)*samp_time; % unit=second
numData=max(data.data(:,15))+1; % +1 because index starts from 0
9 Yaw=data.data(:,12)*pi/180; % radian
ACC_X=data.data(:,4); % unit=1g = 9.8m/s^2
11 ACC_Y=data.data(:,5); % unit=1g = 9.8m/s^2
MK_PITCH=data.data(:,1)/10*pi/180; % radian
13 MK_ROLL=data.data(:,2)/10*pi/180; % radian
stick_pitch=data.data(:,13);
15 stick_roll=data.data(:,14);
g=9.81; % unit 1g
17 %k=0.25; % filter gain
k=0.5; % filter gain
19 desired_v_x=0; % desired velocity along X axis unit=m/s
desired_v_y=0; % desired velocity along X axis unit=m/s
21 Kp=30;
Kd=30;
23
25
27 %Down sampling the x position data because it oversampled.
%The sampling rate of the laser scan matcher is 100ms and the log data is

```

```

29 %sampled at 50ms rate.

31 half_siz = numData/2;
   W_x_100ms= zeros (half_siz ,1);
33 W_y_100ms= zeros (half_siz ,1);
   for i=1 : half_siz
35     W_x_100ms(i) = W_x(i*2-1);
       W_y_100ms(i) = W_y(i*2-1);
37 end

39 %Do interpolation to create smooth graph.
   W_x_=interp (W_x_100ms,2);
41 W_y_=interp (W_y_100ms,2);

43 %Array size align with numData!
   %It's_not_fancy_but_works.
45 W_x_mine=_zeros (numData,1);
   W_y_mine=_zeros (numData,1);
47 for _i=1:_numData-1
   _W_x_mine(i) _=_W_x_(i);
49 _W_y_mine(i) _=_W_y_(i);
   end
51

53 %W_x_mine(1659)=W_x_(1658);
   %W_y_mine(1659)=W_y_(1658);
55

57 %W_v_x=diff (W_x)./ diff (time)

59
%=====
61 %_Step1._Calculate_world_frame_velocity_using_laser_position_data
%=====
63 W_x_v=_zeros (numData, _1);
   W_y_v=_zeros (numData, _1);
65 %for _n=2:numData
   _W_x_v=diff (W_x_mine)/samp_time;
67 _W_y_v=diff (W_y_mine)/samp_time;
   %_W_x_v(n)=(W_x_mine(n)-W_x_mine(n-1))/samp_time;
69 %_W_y_v(n)=(W_y_mine(n)-W_y_mine(n-1))/samp_time;
   _W_y_v(n)=(W_y(n+1)-W_y(n))/samp_time;
71 %end

73
%=====
75 %_Step2._Covert_world_frame_velocity_to_the_body_frame_usnig_rotation
%_matrix
%=====
77
   b_x_v=_zeros (numData, _1);
79   b_y_v=_zeros (numData, _1);
   for _n=1:numData-1
81     _b_x_v(n)=cos (Yaw(n))*W_x_v(n)-sin (Yaw(n))*W_y_v(n);
       _b_y_v(n)=sin (Yaw(n))*W_x_v(n)+cos (Yaw(n))*W_y_v(n);
83   end

85
%=====
87 %_Step3._velocity_complementary_filter
%=====

```

```

89 b_v_hat_x = zeros (numData, 1);
b_v_hat_y = zeros (numData, 1);
91 ddotX = zeros (numData, 1);
ddotY = zeros (numData, 1);
93 b_v_hat_x (1) = 0;
b_v_hat_y (1) = 0;
95
for n = 1 : numData - 1
97 ddotX (n) = -(ACC.X (n) - g * sin (MK.PITCH (n))) / cos (MK.PITCH (n));
ddotY (n) = -(ACC.Y (n) - g * sin (MK.ROLL (n))) / cos (MK.ROLL (n));
99 b_v_hat_x (n + 1) = b_v_hat_x (n) + samp_time * (k * (b_x_v (n) - b_v_hat_x (n)) + ddotX (n));
b_v_hat_y (n + 1) = b_v_hat_y (n) + samp_time * (k * (b_y_v (n) - b_v_hat_y (n)) + ddotY (n));
101 end

103
=====
105 %_Step5. _ Velocity _P _controller
=====
107 pitch_cmd = zeros (numData, 1);
roll_cmd = zeros (numData, 1);
109 error_pitch = zeros (numData, 1);
error_roll = zeros (numData, 1);
111 post_error_pitch = zeros (numData, 1);
post_error_roll = zeros (numData, 1);
113
error_pitch (1) = 0;
115 error_roll (1) = 0;

117 for n = 2 : numData
error_pitch (n) = desired_v_x - b_v_hat_x (n);
119 error_roll (n) = desired_v_y - b_v_hat_y (n);

121 %pitch_cmd (n) = Kp * error_pitch (n) + Kd * (error_pitch (n) - error_pitch (n - 1));
pitch_cmd (n) = Kp * error_pitch (n);
123 %roll_cmd (n) = Kp * error_roll (n) + Kd * ((error_roll (n) - error_roll (n - 1)) / samp_time);
roll_cmd (n) = Kp * error_roll (n);
125 end

127
=====
129 %_Step6. _ Acceleration _integration
=====

131 %for n = 1 : numData - 1
%vel_int_x (n) = samp_time / 2 * (cumsum (ACC.X (n + 1)) + cumsum (ACC.X (n))) * 9.8;
133 %end

135 vel_int_x = cumsum (detrend (ddotX) * samp_time);

137 pos_int_x = cumsum (detrend (vel_int_x) * samp_time);

139

141

143
=====
145 %_Step4. _Plotting
=====

```

```

147 %Create_a_multiline_label_for_the_x-axis_using_a_multiline_cell_array:
149 xlabel({'first line';'second line'})
%Create_a_bold_label_for_the_y-axis_that_contains_a_single_quote:
151 %
ylabel('George's Popularity','fontsize',12,'fontweight','b')
153
155 %=====
%_Fig1._laser_world_position_vs_acc_world_position
157 %=====
figure(1);
159 plot(time,W_x_mine,'r');
xlabel('time [sec]','fontSize',12),ylabel('world position x [m]','fontSize',12);
161 hold_on;
163 plot(time,pos_int_x,'b');
xlabel('time [sec]','fontSize',12),ylabel('world position x from acc_x','fontSize',12);
165
legend('laser world position x','acc world position x');
167 %figure(2);
%plot(time,W_x_v,'b');
169
171 %figure(2);
%plot(time,b_x_v,'m-');
173 %xlabel('time [sec]','fontSize',12),ylabel('body velocity x [m/s]','fontSize',12);
175 %figure(4);
%plot(time,b_y_v);
177
%=====
179 %_Fig2._body_velocity_vs_CF_estimated_velocity
%=====
181
figure(2);
183 plot(time,b_v_hat_x,'r');
xlabel('time [sec]','fontSize',12),ylabel('velocity x [m/s]','fontSize',12);
185
hold_on;
187 plot(time,b_x_v,'b');
189 legend('estimated velocity x','body velocity x');
191 axis([0_time(end)-0.6_0.6]);
%hold_on;
193 %plot(time,vel_int_x,'g');
195 %=====
%_Fig3._pitch_input_vs_stick_pitch
197 %=====
199 figure(3);
plot(time,pitch_cmd,'r');
201 xlabel('time [sec]','fontSize',12),ylabel('pitch cmd vs stick pitch','fontSize',12);
hold_on;
203 plot(time,stick_pitch,'b');
205 legend('pitch cmd','stick pitch');

```



```
207 %figure (7);
    %plot(time,roll_cmd,'r');
209 %xlabel('time [sec]','_','fontsize',12),ylabel('roll cmd vs stick roll','_','fontsize',12);
    %hold_on;
211 %plot(time,stick_roll,'b');

213 %figure (8);
    %plot(time,b_v_hat_y,'r');
215 %xlabel('time [sec]','_','fontsize',12),ylabel('velocity y [m/s]','_','fontsize',12);

217 %hold_on;
    %plot(time,b_y_v,'b');
219 %legend('estimated velocity y','body velocity y');
```